# We are IntechOpen, the world's leading publisher of Open Access books Built by scientists, for scientists

## 6,900
Open access books available

## 185,000
International authors and editors

## 200M
Downloads

Our authors are among the

## 154
Countries delivered to

## TOP 1%
most cited scientists

## 12.2%
Contributors from top 500 universities

BOOK CITATION INDEX
CLARIVATE ANALYTICS
INDEXED

**WEB OF SCIENCE**™

Selection of our books indexed in the Book Citation Index
in Web of Science™ Core Collection (BKCI)

## Interested in publishing with us?
Contact book.department@intechopen.com

Numbers displayed above are based on latest data collected.
For more information visit www.intechopen.com

# Overview of Phosphorus Effect in Molybdenum-Based Hydrotreating Catalysts Supported on Ordered Mesoporous Siliceous Materials

Rafael Huirache-Acuña, Eric M. Rivera-Muñoz,
Trino A. Zepeda, Rufino Nava and Barbara Pawelec

Additional information is available at the end of the chapter

**Abstract**

This chapter presents an overview of the literature on the effect of phosphorus modification of ordered mesoporous silica (OMS) such as MCM-41, HMS, SBA-15, and SBA-16 to be used as supports for hydrotreating catalysts based on transition metal sulfides (TMS). The influence of the support modification with variable quantities of phosphorus on the performance for hydrodesulfurization (HDS) and hydrodenitrogenation (HDN) reactions is outlined and discussed considering the changes in the structural and textural properties ($S_{BET}$), acidity, reducibility, etc., of the substrate brought about by phosphorus incorporation.

**Keywords:** phosphorus, hydrotreating, catalysts, mesoporous, siliceous materials

## 1. Introduction

Heterogeneous catalysts based on transition metal sulfides (TMS) used in the refinery for the hydrotreatment of middle distillates are usually supported on an alumina substrate [1]. This is because alumina is of low cost and shows remarkable textural and mechanical properties [2]. However, as the alumina-supported hydrotreating catalysts display only moderate acidity, it is a common practice to enhance it by surface grafting with $H_3PO_4$ [3]. Besides the enhancement of the support's acidity, the phosphorus might act as a promoter [4]. Unfortunately, alumina-supported catalysts exhibit undesirable strong metal-support interaction (SMSI)

leading to the formation of $AlPO_4$ phase [3]. To overcome this problem, a common practice is phosphatation of the alumina surface which reduces the strong interactions of the molybdenum fraction with the alumina surface [5]. The addition of $H_3PO_4$ to the impregnation solution improves stability and increases metal solubility which enables one to prepare binary Co(Ni)-Mo(W) catalysts in a single impregnation step. Phosphate has been reported to improve the HDS and especially HDN activities of the Mo-based catalysts [3]. The explanations on the beneficial effects of the presence of phosphate validate that phosphate acts as a second promoter [6], decreases the metal-support interactions, improves the solubility of molybdate by the formation of phosphomolybdate complexes which led to easier catalyst preparation [6], inhibits the formation of the inactive $CoAl_2O_4$ or $NiAl_2O_4$ species [5], and favors the formation of the Type-II Co(Ni)-Mo-S structures [7].

The effect of phosphorus strongly depends on P loading, catalyst preparation method, and support chemistry and its morphology [8]. All these factors might explain the controversial catalytic behavior of P-modified Mo-based catalysts in hydrodesulfurization (HDS), hydrodenitrogenation (HDN), and hydrogenation (HYD) reactions. A comprehensive review of the physicochemical processes that occur on the surface of the alumina-supported catalysts modified with phosphorus was carried out by Iwamoto and Grimblot [3]. Recently, the state-of-the art overview of the literature on the effects of phosphorus promotion and poisoning in aluminosilicates (zeolites) was conducted by van der Bij and Weckhuysen [9]. However, to the best of our knowledge, the overview on phosphorus promotion and poisoning in bare silica substrates has not been reported yet. This is probably because compared to alumina-based catalysts, the effect of phosphorus modification of ordered mesoporous silica (OMS) was scarcely investigated [10–17]. Ordered mesoporous silica is a substrate worthy of note as it supports active phases for hydrotreating catalysts. This is because of their interesting textural properties such as a high surface area (above 1000 $m^2\,g^{-1}$), pores in the range of mesopores (2–50 nm), and complementary textural porosity. As the pore wall surface of OMS is carpeted with a high concentration of silanol groups, it can be easy functionalized with different functional groups. As it occurs with alumina-supported catalysts, it was found that the effect of phosphorus modification of the OMS strongly depends on not only P loading but also the method of phosphorus incorporation. Notwithstanding, it is emphasized that the effect of support modification with phosphorus on the catalytic performance is not clearly understood and the activity results are often contradictory. In some cases, the promoting effect of phosphorus on the HDS activity was observed [10–12, 15, 17], while the inhibition effect of phosphorus was found in other studies [16]. OMS exhibits ordered arrangements of channels and/or cavities of different geometries built up from $SiO_2$ units. Their pore size can be controlled and modified, in a reasonable range, using in situ and ex situ synthetic strategies. The effect of P was investigated [11] for the ordered mesoporous silicate, called M41S, which was first synthesized at the Mobil Corporation in 1992 [18]. This material shows a large specific area, a hexagonal array, and uniform pore channels, yet its practical application is limited due to its poor hydrothermal stability. Subsequent to MCM-41, the synthesis of other hexagonal mesoporous materials (HMS) was reported [19, 20]. In comparison to MCM-41, the textural characteristics of the HMS material have certain advantages due, in part, to its larger textural mesoporosity and wormhole mesostructure (*vide infra* **Figure 1**) which offers better transport

for reactants and products [15]. The HMS framework structures, particularly those with a sponge-like particle texture, were claimed to be promising materials for supporting heterogeneous catalysts [12, 21, 22].
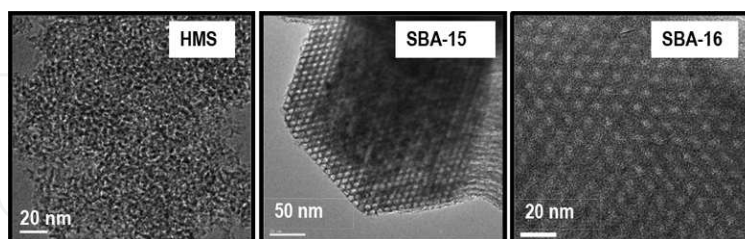


**Figure 1.** HRTEM images of the HMS substrate showing wormhole structure and SBA-15 and SBA-16 substrates displaying highly ordered hexagonal pores in a 2D array.

The more remarkable advance in the synthesis of mesoporous systems was reported by Zhao et al. [23], who synthesized hydrothermally stable mesoporous SBA-15 silica molecular sieves using triblock copolymer surfactants as template. The calcined SBA-15 demonstrated to be more hydrothermally stable than its HMS counterpart with wormhole structure because of its thicker walls with a network of micropores within the walls. The mesoporous SBA-15 has hexagonal pores in a two-dimensional (2D) array with long 1D channels corresponding to the *P6mm* space group symmetry (*vide infra* **Figure 1**). Thus, similar to the case of MCM-41, the parallel channel system of SBA-15 might act as a microreactor, wherein the reactant and the intermediary products will be in prolonged contact with the active phase [2]. In addition to OMS with cylindrical mesopores, the mesoporous silica with a cage-like structure such as SBA-16 has been used for supporting hydrotreating catalysts [24–26]. The siliceous SBA-16 exhibits an *Im3m* space group symmetry (*vide infra* **Figure 1**) with three-dimensional (3D) structure formed by spherical cavities arranged in a body-centered cubic array, which are connected through eight apertures to the nearest neighbors along the (1 1 1) directions [27]. As a consequence, the interconnected spherical mesopores are easily accessible for guest molecules, which facilitate the transport of reactants and products without pore blockage [23, 27].

In this chapter, the effect of phosphate modification of mesoporous silica substrates such as MCM-41, HMS, SBA-15, and SBA-16 on the catalytic response of transition metal sulfide catalysts in hydrotreating reaction has been examined. As most of our conclusions on the effect of OMS modification with phosphorus agree with those discussed recently for aluminosilicates, readers are suggested to study the review by van der Bij and Weckhuysen [9].

## 2. Synthesis of P-containing OMS

Similar to alumina and alumina-silicate-based materials [3, 9], the method of phosphorus introduction was found to play an important role in the distribution of phosphorus in the mesoporous siliceous systems [28, 29]. Two strategies have been undertaken to modify OMS with phosphorus: (i) direct sol-gel, and (ii) post-synthesis methods. For the pure siliceous

substrates, phosphorus incorporation by post-synthesis grafting was more frequently employed than sol-gel synthesis because of its low cost and simplicity.

Direct sol-gel P introduction into OMS was more often employed in medical science applications than in petrochemistry. For example, Vallet-Regi et al. [30] synthesized a P-containing MCM-41 mesoporous material via one-step sol-gel preparation method and then applied as a bioactive material. The characterization of this material by different techniques demonstrated that only a small amount (under 1% P) was incorporated into the structure of MCM-41. The P-containing MCM-41 sample prepared via sol-gel exhibited the characteristic ordered hexagonal array of mesopores of this kind of materials.

Direct sol-gel synthesis was also employed by Pitchumani et al. [28] for the preparation of the SBA-15 substrates with distinct morphologies (well-ordered mesoporous films, cakes, fibers, and bundle-like structures). In general, the synthesis of the SBA-15 substrate involves the formation of organic-inorganic composites by a self-assembly process in which the organic phase serves as a template for the inorganic phase [23]. In this process, tetra-ethyl orthosilicate (TEOS) is used as silica source, and a nonionic P123 block copolymer as surfactant ($EO_{20}$-$PO_{70}$-$EO_{20}$, where EO is ethylene oxide and PO is propylene oxide) and a self-assembly of both phases occurs in the presence of strong acids such as HCl.

With the aim to elucidate the reaction between the phosphate ions and silica species, Tagaya et al. [29] investigated the influence of the P incorporation methodology (coating vs. doping) on the nanostructure of phosphorus-containing mesoporous silica films. Phosphoric acid was added before and after the mesopore formation (doping and coating methods, respectively). In the coating method, the calcined mesoporous silica film was spin-coated with an aqueous solution of $H_3PO_4$ at four different rotation speeds and then calcined at 450°C for 6 h. It was observed by XRD that the films prepared by the coating method exhibited high-ordered pore channels with a hexagonal structure parallel to the substrate surface, while those prepared by doping method exhibited larger pores with worm-like structures. This could be explained considering that the coating method leads to the interaction of $H_3PO_4$ with the silica species. In such cases, the P-O-Si bonds can be formed during hydrogenolysis, while the hydroxyl groups of phosphoric acid can be eliminated by calcination. Besides, the hydroxyl groups on phosphorus species can be restored by exposing the calcined sample to an air mixture [28]. In the doping method, an aqueous solution of phosphoric acid is added instead of HCl during the mesoporous silica film preparation (one-pot synthesis). In such cases, a larger amount of $H_3O^+$ and phosphate ions could be adsorbed on the hydrophilic head groups of the cationic surfactant of cetyltrimethylammonium chloride (CTAC) leading to the formation of Si-O-P-OH groups [29].

Using the post-synthesis method, phosphorus could be grafted onto the surface of silica materials by treating with phosphoric acid for a very short time, followed by high-temperature calcination [31]. This method was employed by many researchers. For example, it was used for phosphorus incorporation onto the surface of SBA-16 [25], HMS [15], Al-HMS [22], MCM-51, and SBA-15 substrates [9]. Using the post-synthesis grafting method for phosphorus introduction, the bare mesoporous silica substrate is synthesized first and after its calcination, the pure siliceous material is made to be in contact with an aqueous solution of

$H_3PO_4$ having an appropriate concentration of phosphoric acid. After drying, the obtained materials are calcined. For example, for the preparation of P-containing HMS, the $S°I°$ assembly of HMS molecular sieve silica with wormhole framework structures can be accomplished using dodecylamine (DDA) as the structure-directing surfactant ($S°$) and tetra-ethyl orthosilicate (TEOS) as the inorganic precursor ($I°$) [32]. The procedure similar to that reported by Zhang et al. [23] was employed by Nava et al. [15] for the preparation of pure siliceous HMS material. After solid calcination at 813 K for 6 h, the P-modified HMS was prepared by making the parent HMS come in contact with an aqueous solution of $H_3PO_4$ (incipient wetness impregnation). Then, the solid was dried at 383 K overnight and then calcined at 773 K for 3 h under static conditions. In the case of the P-containing HMS-Al, the parent Al-HMS substrate (Si/Al molar ratio of 40) was prepared by Zepeda et al. [22] following the procedure described by Gontier and Tuel [33].

Finally, another variation of the post-synthesis method for P-incorporation is the simultaneous impregnation of the bare support with metal salt precursors and $H_3PO_4$. This method, which is commonly used for the manufacture of HDS catalysts at commercial scale, was employed by Hernández et al. [34] for the preparation of Co-Mo-P/Al-MCM-41 catalysts.

## 3. Influence of phosphorus on morphology of OMS materials

In general, the incorporation of phosphate on the OMS substrates by post-synthesis grafting method does not change their structure, as it was confirmed by comparison of small-angle XRD patterns of the P-loaded and unloaded HMS [15 ,21], SBA-15, and SBA-16 [24]. This is probably because the separate $P_2O_5$ phase could be formed during calcination of the acid-functionalized solids having $-PO_3H$ or $-PO_2H$ groups formed through interaction of the P-OH bonds of $H_3PO_4$ and the surface silanols [31]. These phosphate species remain deposited as a separate phase on the surface of OMS substrates, as it was confirmed for P/HMS systems by Nava et al. [15]. This is not the case of more reactive alumina for which phosphate reacts to a large extent on the surface layers of the alumina forming a well-dispersed $AlPO_4$ phase [6, 35]. In the case of P incorporation on the surface of calcined Ti-HMS, the textural and surface properties of HMS were modified by Ti cations incorporated during one-pot synthesis. The physical and chemical characterization of such calcined substrates indicated that the presence of phosphorus pentoxide species on the support surface does not change the mesoporous character of the HMS-Ti substrate, but modifies its surface properties [21]. The P/HMS-Ti substrates, which were prepared by wet impregnation of HMS-Ti substrate with $H_3PO_4$ followed by calcination at 500°C, exhibited almost a linear decrease in the specific surface area ($S_{BET}$) with increasing P loading. This is because of blocking of some support pores by $P_2O_5$ species located almost exclusively on the external support surface, as demonstrated by calculation of the normalized BET surface area [21]. A higher concentration of phosphorus species on the zeolite surface compared to phosphorus in the bulk was also reported for the P-modified zeolites, wherein the introduction of phosphoric acid into a zeolite was made by wet impregnation [36–38]. This is because dehydration occurring during heat treatment leads to the formation of large condensed polyphosphate and $P_2O_5$ species [35]. This is in good

agreement with the results of the P-modified zeolites [9]. The majority of these phosphorus species exhibited no interaction with mesoporous silica, which are considered as separate phases [16, 17, 21]. Using the small-angle X-ray powder diffraction technique, Zepeda et al. [21] confirmed that all P($x$)/HMS-Ti substrates modified with small amounts of P (0.2–1.2 wt. % of $P_2O_5$) exhibited single small-angle reflection corresponding to the (100) plane, which is characteristic of the HMS material. Although higher-order Bragg reflections were not observed in the patterns of S°I° HMS materials, the single $d_{100}$ peak indicates that all materials display a short-range hexagonal symmetry with a uniform pore diameter. A similar XRD pattern was reported for the HMS-Ti system [33]. For the P-free HMS-Ti substrate, the small-angle reflection is located at $2\theta = 1.30°$. After P loading onto the surface of HMS-Ti, the $d_{100}$ peak is shifted to higher angles (from 1.30 to 1.38°). The calculation of the wall thickness indicates a slight decrease in this parameter after addition of P to HMS-Ti (from 4.27 to 3.92 nm). This may indicate that impregnation of HMS-Ti substrate with $H_3PO_4$ led to a lattice reduction and a decrease in pore diameter. Indeed, the unit cell parameter ($a_0$) calculated using the equation $a_0 = 2d_{100}/\sqrt{3}$ indicated that support modification with phosphorus produced a slight decrease in the unit cell parameter (from 7.67 to 7.12 nm) [21]. Similar to the phosphorus effects, an increase in the pore diameter might occur if the catalyst is prepared by the simultaneous impregnation method as compared with that prepared by the successive impregnation [13]. This is deduced from **Figure 2** which shows the XRD patterns of the HMS-based catalysts prepared by simultaneous and successive impregnation. As seen in this figure, the oxide precursors prepared by simultaneous and successive impregnation methods exhibit their $d_{100}$ peaks around 1.14 and 1.34° in $2\theta$, thus suggesting an increase in the dimensions of the scattering domain, and in consequence, an increase of the pore diameter for the samples prepared by simultaneous impregnation [13].
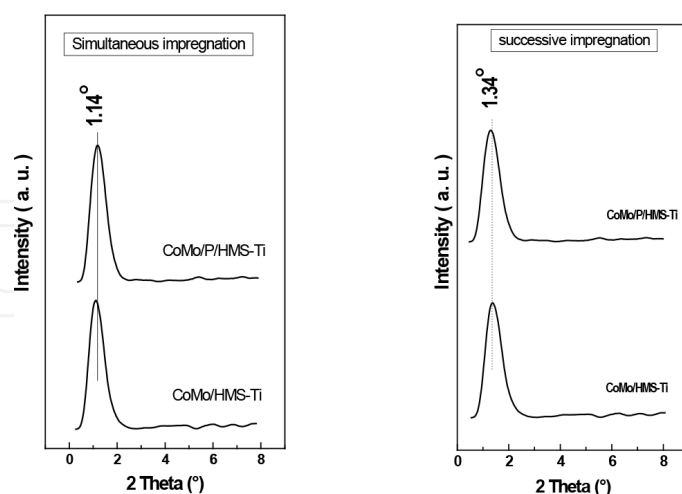


**Figure 2.** Low-angle X-ray diffraction patterns of the oxide precursors of CoMo/HMS-Ti and CoMo/P/HMS-Ti catalysts prepared by successive and simultaneous impregnation methods [13] (reproduced with permission from Elsevier).

Similar to the P/HMS-Ti-based catalysts [13, 21], P incorporation on the surface of SBA-15 by post-synthesis grafting did not lead to significant changes in the small-angle XRD patterns of

the P/SBA-15 substrates [24]. Moreover, similar to the HMS-based substrates [21], the diffraction peaks of the P-loaded SBA-15 samples were shifted to larger $2\theta$ values with respect to bare SBA-15 samples, thereby indicating that the P-loaded sample shows smaller unit cell parameter than the unloaded one [24]. This means that when phosphoric acid was added to SBA-15, the structural integrity of the mesoporous silica decreased upon increasing the amount of grafted acid. For very low P loading, the uniformly arranged hexagonal mesoporous framework was preserved. Indeed, Shon et al. [39] observed that the hexagonal mesoporous framework of SBA-15 substrate was maintained even after loading of excess of $H_3PO_4$ onto the surface of this material (Si/P ≈ 10).

## 4. Changes in textural properties of OMS induced by phosphorus

In general, textural characterization of the P-containing mesoporous silica from the $N_2$ adsorption-desorption isotherms indicated that P loading by post-synthesis grafting has a detrimental effect on their textural properties, as demonstrated for the P/HMS and P/HMS-Al prepared by grafting the respective parent substrate with $H_3PO_4$ [17, 22], The observed decrease in the specific BET surface area and pore volume was explained in terms of a partial blockage of the pores by the P species. Similarly, P loading onto siliceous MCM-41 by post-synthesis grafting method caused a deterioration of the textural characteristics and some loss in the periodicity of the MCM-41 pore structure [11]. In order to understand the mechanism of such alteration, the stability of various structured mesoporous materials (SBA-1, SBA-3, SBA-15, MCM-41, and MCM-48) under acidic conditions of $H_3PO_4$ was investigated [40]. These authors reported that the micropores were first damaged, and then the mesopores were partially collapsed or partially blocked. The resistance of the material against acidic media was associated with a critical wall thickness-pore diameter threshold. Contrary to the grafting method [22], the P incorporation by direct sol-gel synthesis method led to an increase in the specific surface area and pore volume of mesoporous silica substrates for the mesostructurated P-doped silica monoliths. As the P-loaded monolith exhibited a smaller average pore size and unit cell parameter than its unloaded counterpart, the observed increase of specific surface area and pore volume was explained due to the formation of disordered and interconnected pores inside each microdomain [41].

Hexagonal mesoporous HMS (Si/Ti molar ratio of 40) modified with both Ti and P were used as supports for Co(Ni)Mo sulfide phases by Zepeda et al. [21]. The Ti-loaded HMS (Si/Ti molar ratio of 40) was prepared by direct synthesis, wherein the titanium precursor was added to the synthesis gel. After calcination, the $Ti^{4+}$ ions were incorporated into the framework of the HMS substrate. The P-containing supports were prepared by typical impregnation of the calcined HMS-Ti substrate with an aqueous solution of $H_3PO_4$. Investigation of textural properties of the bare supports demonstrated that Ti insertion into the framework of HMS did not change the mesoporous character but modified the surface properties even though the low-angle XRD patterns demonstrated almost no changes in pore ordering upon P loading and/or preparation procedure [13]. Contrary to P/Ti-HMS [21], the $N_2$ adsorption-desorption and small-angle XRD measurements of the HMS modified with both Al and P confirmed a decrease

of specific surface area and partial destruction of the support mesoporous structure after modification of calcined Al-HMS with phosphorus [12, 22].

## 5. Metal oxides formed on the support surface modified with P

It is well known that the dispersion and structure of Mo species is a consequence of the modification of the substrate's isoelectric point and a change in the interaction of the adsorption of molybdate species during the impregnation procedure. Thus, depending on the acid concentration, the support impregnation with $H_3PO_4$ might change the isoelectric point of the support, thereby influencing the interaction of the molybdate species with support. In addition, the ordered framework of the OMS may control the metal oxide particle size limiting the growth of the clusters introduced into the confined space of the channels. Thus, the presence of phosphate species on the support surface might influence the metal oxide location of the phases formed. In this context, the XRD, DRS, and TPR characterizations of the Ni/Mo/P/MCM-41 oxide precursors by Herrera et al. [11] showed that the characteristics (dispersion, coordination state, and temperature of reduction) of oxide Mo and Ni species changed with phosphorus incorporation in the MCM-41.

The influence of phosphorus species on the formation of metal oxide phases on the support surface was investigated by Nava et al. [15, 17]. The X-ray diffraction patterns of the calcined catalysts confirmed the formation of the crystalline $MoO_3$ phase (JCPDS 5-508) and β-$CoMoO_4$ phase (JCPDS 21-0868). Considering the crystal size of the β-$CoMoO_4$ phase, these authors concluded that the catalysts with low P loading exhibited higher dispersion of Co and Mo phases than their counterparts having high P loadings. The catalyst modified with the largest P loading displayed the largest crystal size of the β-$CoMoO_4$ phase (14.2 nm). This was explained in terms of the decrease of the metal-support interaction induced by a large amount of phosphate species located on the support surface [17]. The wide-angle XRD diffraction technique was employed by Pawelec et al. [13], for characterization of the oxide precursors of CoMo/P/HMS-Ti catalysts prepared by simultaneous and successive impregnation methods. All the samples prepared by simultaneous impregnation did not show reflections belonging to cobalt and molybdenum oxide, suggesting that the phases formed are amorphous or not fully crystalline, or their crystal sizes are below the detection limit of the XRD technique. By contrast, the XRD diffraction patterns of the catalysts prepared by simultaneous impregnation exhibited a small reflection peak at 22.7° 2θ and an intense reflection peak at 25.7° 2θ, overlapping with a broad diffraction of the substrate, which are due to crystalline $MoO_3$ phase (JCPDS card 1-076-1003). The intensity of both reflections increased suggesting a higher preference of molybdenum ions for P-OH groups of P(x)/HMS-Ti support than for cobalt [42].

## 6. Effect of phosphorus on the formation of active sites

As mentioned in Section 1, the effect of phosphorus on the HDS activity of catalysts depends on the P loading. The effect of support modification by phosphorus on the morphology of $MoS_2$

and "Co(Ni)-Mo(W)-S" type structures formed after precursor sulfidation was largely investigated. As the most active catalysts in HDS reaction are mixed "Co(Ni)-Mo(W)-S" structures, the main question arises: ***May the separate phosphate species located on the support surface influence the formation of "Co(Ni)-Mo-S" active phases?*** The most intuitive explanation for the phosphorus inhibition of HDS reaction over supported Co(Ni)Mo(W) catalysts is that the phosphorus species may act as a physical barrier inhibiting the formation of this phase. However, surface analysis by XPS of fresh sulfided CoMo/HMS and CoMo/P/HMS catalysts by Nava et al. [16] strongly suggested that the catalyst preparation method should be more important for the formation of the mixed "Co-Mo-S" phase than the presence of phosphate species on the support surface. Both CoMo/HMS and CoMo/P/HMS sulfide catalysts showed the S 2p peak characteristic of $S^{2-}$ ions (binding energy (BE) of $161.2 \pm 0.1$ eV). For the CoMo/P/HMS sulfide catalyst, the P 2p peak (BE at 134.0 eV) was indicative of the presence of phosphate species on the support surface. Moreover, the Mo $3d_{5/2}$ core-level spectra appeared at binding energy characteristic of $MoS_2$ phase (BE at 228.7 eV) and the Co $2p_{3/2}$ core level spectra showed two contributions, one due to the formation of $Co_9S_8$ phase (BE at 778.2–778.8 eV) and another due to non-sulfided $Co^{2+}$ species (BE at 780.2–780.8 eV). Taking into account these XPS data of both P-containing and P-free catalysts, the formation of "CoMoS" phase is precluded. Thus, it is impossible to conclude that phosphate species on the support surface does not inhibit the formation of this phase. Although the formation of "Co-Mo-S" phase did not occur, the sulfide CoMo/P/HMS catalyst showed surface exposure and sulfidation degree larger for both cobalt and molybdenum than on its P-free counterpart. Thus, the presence of the phosphate species on the support surface enhanced the surface exposure of $MoS_2$ particles, in close agreement with the HRTEM characterization data [16].

The genesis of the active phases formed during sulfidation of $Ni/P/SiO_2$ catalysts with $H_2/H_2S$ gas mixture was studied by Koranyi [10]. Under the reaction conditions, the P-containing catalysts exhibited a higher HDS activity than the P-free sulfided $Ni/SiO_2$. The increase in activity observed for P-containing catalysts was linked with the formation of both nickel sulfide and nickel phosphide phases during catalyst activation during sulfidation. The larger intrinsic activity of the nickel phosphide with respect to nickel sulfide is linked with its different structure. Contrary to the metal sulfides, the structure of the metal phosphides is based on trigonal prisms having large phosphorus atoms (atomic radius of phosphorous is 0.109 nm) located in their centers. Importantly, contrary to the transition metal sulfides, transition metal phosphides do not exhibit a layered structure, which offers potentially better exposure of surface atoms to reactants [43]. The work by Koranyi [10] demonstrated that the simple impregnation procedure was suitable to bring at least part of the nickel in close contact with phosphorus. Contrary to $Ni/P/SiO_2$, the activity of P-free $Ni/SiO_2$ catalyst was associated with the nickel sulfide surface area, as confirmed by dynamic chemisorption measurements (DOC). In addition, Koranyi [10] observed that the catalyst presulfided at atmospheric pressure was more active than its counterpart sulfided at an elevated pressure. This result suggests that the type of active phases formed (nickel sulfides or nickel phosphides) depends on the $H_2/H_2S$ gas pressure employed for catalyst sulfidation. The ability of phosphorus to modify the morphology of the $Mo(W)S_2$ phase has been observed for sulfided NiMoW/SBA-16 catalysts modified with phosphorus by Guzmán et al. [25]. In the light of HRTEM

results, the low HDS activity of P-free NiMoW/SBA-16 sample was explained on account of the development of poorly active "onion-type" Mo(W)$_2$ structures (see **Figure 3**). This was also confirmed by HRTEM investigation by Herrera et al. [11] on the morphology of MoS$_2$ phase formed on the surface of sulfided NiMo/P/MCM-41 catalyst loaded with a low amount of phosphorus (2 wt.% P$_2$O$_5$). HRTEM images indicated the formation of small MoS$_2$ crystallites (0–6 nm) with two or three layers. For these catalysts, an increase of P loading from 2.0 to 5 wt.% led to an increase in the average length and layer stacking of MoS$_2$ crystallites.
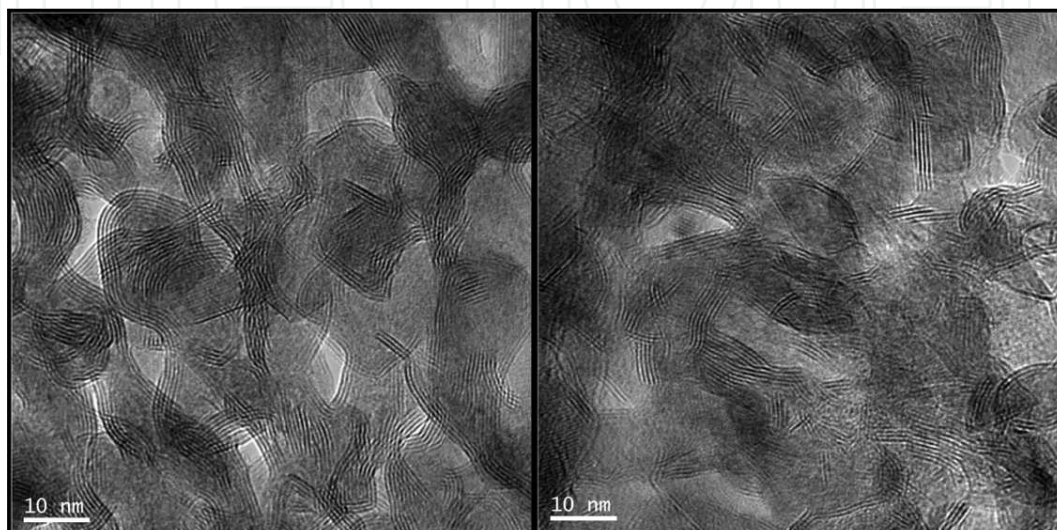


**Figure 3.** HRTEM images showing the enhancement of the active phase dispersion on the fresh sulfided NiMoW/P/SBA-16 catalyst modified with P with respect to P-free NiMo/SBA-16 (left) (adapted from Guzman et al., [25], with permission of Elsevier).

## 7. Effect of phosphorus addition on acid sites

The naked mesoporous silicas exhibit electronically neutral framework and lack of Brønsted acidity. As bifunctional catalysts having both metal and acid functions are required for hydrotreating reactions, the formation of Brønsted acid sites on the surface of mesoporous silicas is very important for their potential application as supports of the hydrotreating catalysts. For instance, the bifunctional catalysts are required for the reaction of dehydration of isopropanol [31], hydrodesulfurization of 4,6-Dimethyldibenzothiophene (4,6-DMDBT) [17, 22], and hydrodesoxygenation of anisole [26]. To circumvent this limitation, many approaches have been undertaken, among which the substitution of Si$^{4+}$ by different cations, functionalization with different groups, carrying the preparation method or changing the active phase component remain prominent [44]. In order to control both acid strength and acid site density, functionalization of the silica surfaces with various kinds of organosilane compounds was the most commonly employed methodology [39].

Pitchumani et al. [28] employed a weak acid (H$_3$PO$_4$) instead of strong HCl acid during the direct synthesis of P-containing SBA-15 substrates. Assuming the interaction of H$_3$PO$_4$ on the

silica surface which leads to phosphorus incorporation into the silica framework, Brønsted acid sites are expected to occur. Unfortunately, no experimental evidence of the formation of the Si-O-P bonds was reported. Similarly, Shon et al. [39], claimed the formation of Brønsted acid sites on the SBA-15 catalysts during interaction of the $H_3PO_4$ at the silica surface. SBA-15-based catalysts were functionalized with -$PO_3H_2$ groups by post-grafting with $H_3PO_4$, followed by drying in a vacuum oven at 60°C for 12 h and then by calcination at 500°C for 4 h under static air conditions. The latter process led to the decomposition of phosphorus precursors into (poly)phosphates and phosphorus pentoxide.

Unfortunately, in the studies by Pitchumani et al. [28] and Shon et al. [39], there is no experimental evidence on the formation of those bonds. The same situation occurs in the case of the microporous aluminosilicates [9]. On the contrary, there is experimental evidence on the formation of Lewis acid sites as it was demonstrated by the FTIR spectra of adsorbed pyridine for freshly sulfided P-loaded CoMo/HMS catalysts [15]. Interestingly, the temperature-programmed desorption patterns of desorbed ammonia performed on the oxide precursors of these catalysts demonstrated that the phosphate phase remained on the surface of HMS. These phosphate moieties are responsible for the formation of weak acid sites whose proportion increases with increasing P loading on the substrate [15]. This is in good agreement with the work by Wang et al. [45] who observed that relatively more strong and medium strength acid sites are affected by phosphatation than weak acid sites [17]. Calcined CoMo/HMS catalysts loaded with variable amounts of phosphorus (0.5, 1.0, 1.5, and 2.0 wt.% of $P_2O_5$) were characterized by $^{31}P$ NMR spectroscopy by Nava et al. [17]. The $^{31}P$ NMR spectra indicated that the catalyst with the lowest P loading exhibited isolated phosphate units, whereas the one with $P_2O_5$ loading of 1.5 wt.% shows the phosphorus atoms connected to silica forming the O=P(OP/OSi) linkages. The catalysts with $P_2O_5$ loading of 1.0 and 2.0 wt.% resulted in the formation of P-OH groups. In no case, phosphomolybdate complexes were formed.

The effects of modification of the SBA-16 surface with variable amounts of phosphorus on the acidity of oxide catalyst precursors and sulfided catalysts were investigated by the $NH_3$-TPD technique by Guzman et al. [25]. It was found that, regardless of the pretreatment, all P-containing samples show larger acidity than the P-free counterpart. The formation of $P(OH)_2$-O-Si bonds, or even free $OP(OH)_3$ entities interacting with the surface via H-bonding, during the support modification with phosphoric acid was proposed by Lewis et al. [46, 47] and Kawi et al. [31]. However, the theoretical calculation indicated that the formation of Si-O-P bonds could be excluded because they are very unstable [48].

The lowering of acidity after support grafting with a large amount of -$PO_3H_3$ groups observed by Guzman et al. [25] for NiMoW/P1.0/SBA-16 catalyst loaded with 1.0 wt.% of $P_2O_3$ (*vide infra* **Figure 4**) might indicate that a critical concentration of phosphoric acid is able to react with the surface hydroxyl groups. Above this critical concentration, $H_3PO_4$ reacts not only with the Si-OH groups but also with the P-OH groups to form polyphosphate species [46, 47]. Indeed, the XPS data analysis of those catalysts revealed that the binding energy of $P_{2p}$ level of P-containing catalysts was much lower than those corresponding to $P_2O_5$ (134.0 vs. 135.2 eV) and similar (133.5 eV) to that reported for Si-MCM-41 grafted with -$PO_3H_2$ or -$PO_2H$ groups [31].
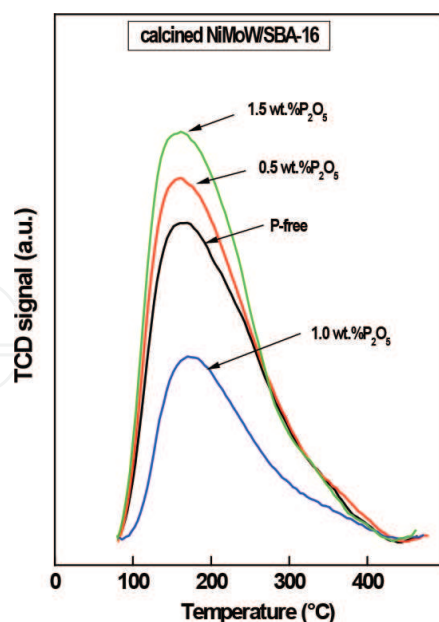
**Figure 4.** TPD-NH$_3$ profiles of oxide NiMoW/P($x$)/SBA-16 catalyst precursors ($x$ = 0.5–1.5 wt.%).

Moreover, it is known that the catalyst sulfidation led to a further increase in the catalyst acidity due to the formation of the -SH groups attached to the support surface [25]. However, among the catalysts loaded with different P contents, the sulfided NiMoW/P/SBA-16 catalysts with 1 wt.% P showed greater total acidity than its P-free counterpart, which may explain in part its best catalytic performance. On the contrary, the lower acidity of NiMoW/P/SBA-16 sulfide catalyst with a low P loading (0.6 wt.%) with respect to the P-free catalyst was explained in terms of the limited accessibility of ammonia to some acid sites due to the presence of small metal sulfide particles located on the substrate pores.

The increase of the catalyst acidity by support modification with phosphorus was also confirmed for NiMo/P/HMS-Al systems by Zepeda et al. [12, 22]. Their P-containing samples exhibited a greater acidity than their P-free counterpart, as confirmed by TPD-NH$_3$ study of oxide precursors and by DRIFT and FT-IR studies of adsorbed pyridine on the fresh sulfided catalysts.

## 8. Influence of phosphorus on the catalytic performance

The influence of phosphorus on the catalytic performance of transition metal sulfides was investigated in different hydrotreating reactions such as HDS, HDN, HDS+HDN, HDO, and HYD is shown in **Table 1**. Some reports showed that phosphorus acts as a promoter, while in many others, it was found to act as an inhibitor. Indeed, the most widely tested reaction to probe the performance of P-loaded silica was the HDS of dibenzothiophene (DBT). This is because DBT is a typical sulfur-containing molecule present in the petroleum fraction of high-boiling point or coal-derived liquids. Moreover, it is expected that DBT molecule did not show any diffusion limitation to access the porous structure of the mesoporous siliceous materials

because this molecule covers a surface area of 8.0 × 12.2 Å$^2$. As compared to the DBT mole-cule, it is more difficult to desulfurize the alkyl-substituted DBTs, especially when both alkyl groups are in the 4- and 6-positions. Although the exact origin of the difficulty of converting alkyl-substituted DBTs using conventional alumina-supported Co(Ni)Mo catalysts still remains unclear, current studies associate this with (i) steric hindrance of the C-S bond scission in the adsorbed sulfur compound, (ii) the availability of only one H atom in the elimination step, and (iii) the influence of the alkyl group on the acidity of the H atom. The activity results for the HDS of 4,6-DMDBT confirmed that this reaction over CoMo/P/HMS-Ti sulfide catalysts proceeds via dealkylation and isomerization reaction pathways [13, 14]. The simplified reaction scheme for the HDS of 4,6-DMDBT reaction over those catalysts is shown in **Scheme 1**. In the HDS of DBT reaction, the DBT transformation occurs through parallel direct desulfur-ization (DDS) and hydrogenation (HYD) pathways: DDS route of DBT transformation leads to the formation of biphenyl (BP) via hydrogenolysis, whereas the HYD of one and two aromatic rings of DBT leads to the formation of tetrahydrodibenzothiophene (THDBT) and cyclohexylbenzene (CHB), respectively (see **Scheme 1**).
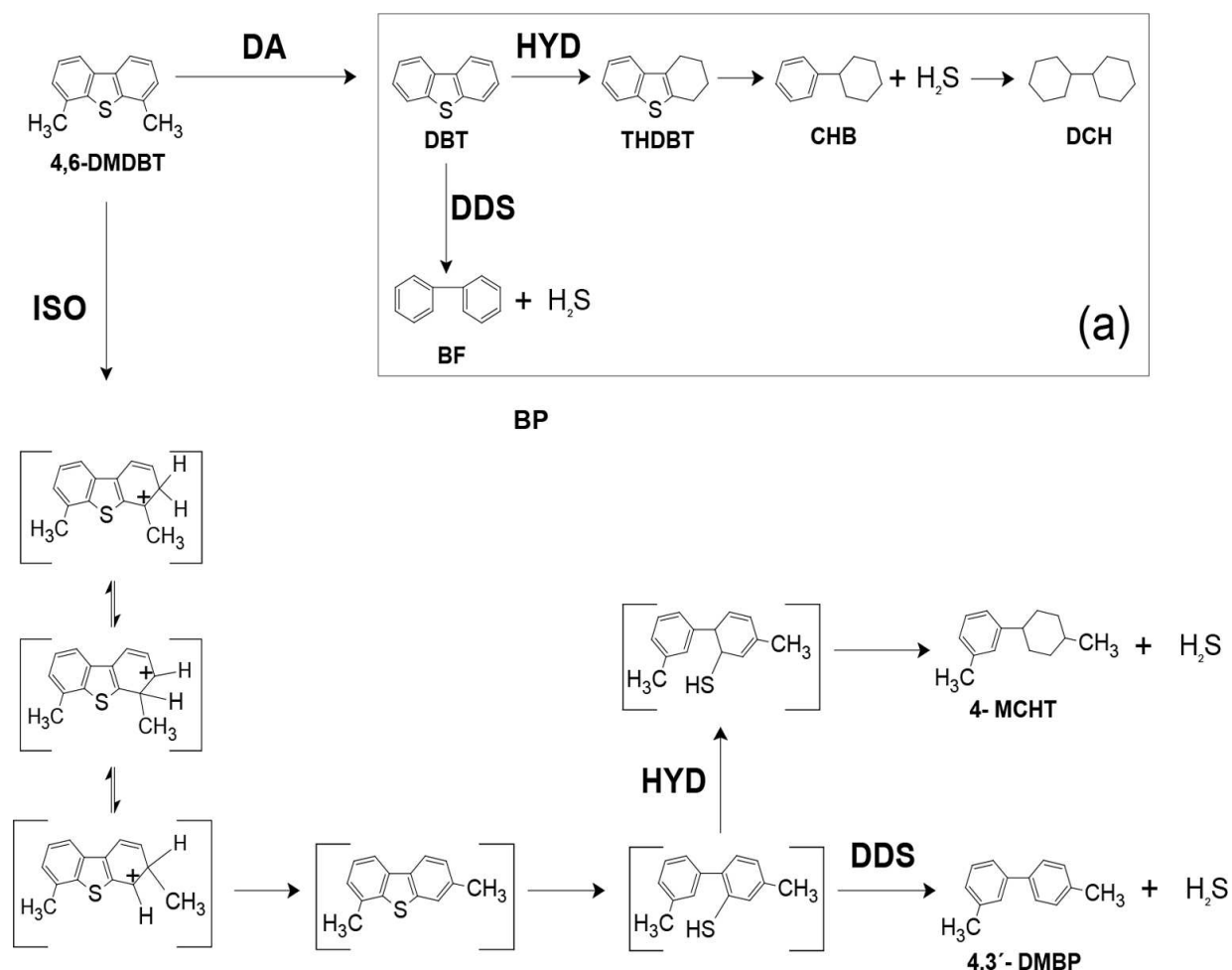


**Scheme 1.** Simplified reaction's schemes for the HDS of 4,6-DMDBT molecule based on the work of Nava et al. [17] (adapted with permission from Elsevier).

| Catalyst[a] | Reactant | Reaction conditions | Reference |
|---|---|---|---|
| **Phosphorus promotion effect** | | | |
| Ni/P/SiO$_2$ | Thiophene | Flow reactor, $T$ = 673 K; $P$ = 1 bar | Korányi [10] |
| NiMo/P/MCM-41 | DBT, 4,6-DMDBT | Batch reactor, $T$ = 573 K, $P$ = 7.3 MPa | Herrera et al. [11] |
| CoMoP/Al-MCM-41 | DBT | Batch reactor, $T$ = 593 K, $P_{H2}$= 5.6 MPa | Hernández et al. [10] |
| Co/Mo/P/HMS | DBT | Batch reactor, $T$ = 623 K, $P$ = 3.1 MPa | Nava et al. [15, 17] |
| CoMo/P/HMS | DBT | Batch reactor, $T$ = 623 K, $P$ = 3.1 MPa | Nava et al. [15] |
| CoMo/P/HMS | 4,6-DMDBT | Flow reactor, $T$ = 583 K, $P$ = 5.0 MPa | Nava et al. [17] |
| CoMo/P/HMS-Ti | DBT | Batch reactor, $T$ = 593 K, $P$ = 5.5 MPa | Pawelec et al. [13] |
| CoMo/P/HMS-Ti; Co/Mo/P/HMS-Ti | 4,6-DMDBT | Batch and flow reactors, $T$ = 598 K, $P$ = 5.5 MPa | Pawelec et al., [14] |
| CoMo/P/HMS-Ti | DBT | Batch reactor, $T$ = 593 K, $P$ = 5.5 MPa | Zepeda et al. [21] |
| NiMo/P/HMS-Al | Thiophene, 4,6-DMDBT | Batch reactor, $T$ = 593 K, $P$ = 5.5 MPa | Zepeda et al., [22] |
| NiMo/P/HMS-Al | DBT | Batch reactor, $T$=593 K, $P$=5.5 MPa | Zepeda et al. [12] |
| NiMo/P/HMS-Al | Carbazole | Batch reactor, $T$ = 593 K, $P$ = 5.5 MPa | Zepeda et al. [12] |
| NiMo/P/HMS-Al | DBT+ carbazole | Batch reactor, $T$ = 593 K, $P$ = 5.5 MPa | Zepeda et al. [12] |
| NiMoW/P/SBA-16 | DBT, 4,6-DMDBT | Batch reactor, $T$ = 593 K, $P$ = 5.0 MPa | Guzman et al. [25] |
| **Phosphorus inhibition effect** | | | |
| Co/Mo/P/HMS | DBT | Batch reactor, $T$ = 623 K, $P$ = 3.1 MPa | Nava et al. [15, 16] |
| NiMo/P/HMS-Ti; NiW/P/HMS-Ti | Naphthalene | Batch reactor, $T$ = 598 K, $P$ = 7.7 MPa | Halachev et al. [49] |
| CoMoW/P/SBA-15 | DBT | Flow reactor, $T$ = 623 K, $P$=3.1 MPa | Huirache-Acuña et al. [24] |
| CoMoW/P/SBA-15 | Anisole | Flow reactor, $T$ = 583 K, $P$ = 3.0 MPa | Loricera et al. [26] |
| CoMoW/P/SBA-16 | DBT | Flow reactor, $T$ = 623 K, $P$ = 3.1 MPa | Huirache-Acuña et al. [24] |
| CoMoW/P/SBA-16 | Anisole | Flow reactor, $T$ = 583 K, $P$ = 3.0 MPa | Loricera et al. [26] |

[a] Co/Mo (Ni/Mo): the catalysts prepared by successive impregnation; CoMo (NiMo): the catalysts prepared by simultaneous impregnation; CoMoP: simultaneous impregnation with metal salt precursors and H$_3$PO$_4$.

**Table 1.** Overview of the influence of phosphorus on the catalytic performance.

## 8.1. Effect of phosphorus concentration

A study reported by Nava et al. [50] clearly showed that the addition of phosphorus during preparation of unsupported NiMoW catalysts has detrimental effects on both textural and performance characteristics. The authors attributed the loss of activity to the loss of the Ni promotional effect resulting from the stronger interaction of P with Mo and W than with Ni. Moreover, the HRTEM results suggested that the proportion of Mo(W)S$_2$ slabs was drastical-

ly reduced after phosphorus addition. Contrary to the unsupported NiMoW, both inhibition and promotional effects were observed for the hydrotreating catalysts supported on the OMS substrates. An overview of the phosphorus effect for hydrotreating reactions is compiled in **Table 1**. It can be emphasized that most of the studies reporting the promotional effect of P were concentrated on the HDS reactions of transition metal sulfides.

The positive effect of P loading on the HDS activity of bifunctional NiMo catalysts supported on MCM-41 substrates was reported by Herrera et al. [11]. The surface of the MCM-41 substrate modified with variable amounts of phosphorus (0–5 wt.% $P_2O_5$) was prepared by post-synthesis grafting. In good agreement with the study by Guzman et al. [25], it was found that the modification of MCM-41 with phosphorus results in high-performance NiMo catalysts, especially for the HDS of DBT reaction. Regardless of the reaction, the promotion of the hydrogenation pathway of HDS reaction occurs. This was explained in terms of the changes in the morphology of $MoS_2$ active phase induced by phosphorus. Surprisingly, the P-containing catalysts exhibited a higher catalytic activity in 4,6-DMDBT HDS than in DBT HDS reaction, with all P-containing catalysts being more active in the 4,6-DMDBT HDS reaction than a commercial NiMo/$Al_2O_3$ catalyst. Maximum catalytic activity in HDS of 4,6-DMDBT reaction was observed for the catalyst supported on MCM-41 modified with 1 wt.% $P_2O_5$.
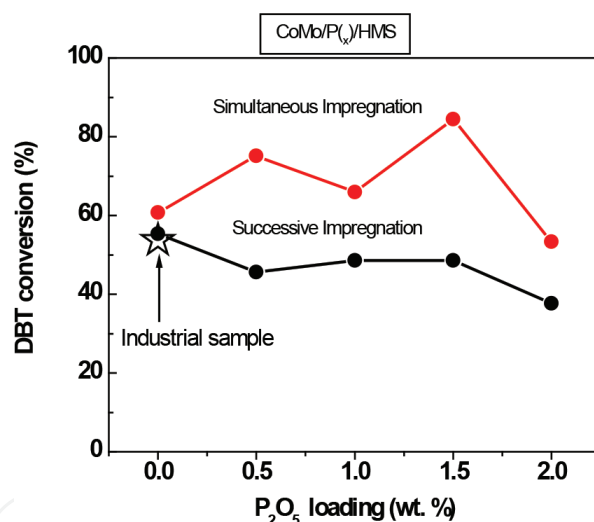


**Figure 5.** Influence of P loading and catalyst preparation method (successive impregnation vs. simultaneous impregnation) on the activity of CoMo/HMS sulfide catalysts in HDS of DBT. As reference, the DBT conversion data of an industrial sample is included (adapted from Nava et al. [15] with permission from Elsevier).

The influence of P loading on the HDS activity of P-containing CoMo/P/HMS sulfide catalysts prepared by sequential and successive impregnation was investigated by Nava et al. [15]. Their P-containing substrates were prepared by incipient wetness impregnation of the parent HMS support with an aqueous solution of $H_3PO_4$ having an appropriate concentration to obtain P/HMS supports with $P_2O_5$ loading in the range of 0.5–2.0 wt.%. **Figure 5** shows that the P effect is not linear and strongly depends on the method of catalyst preparation. The best HDS activity was shown by the catalyst loaded with 1.5 wt.% of $P_2O_5$ which was prepared by simultaneous impregnation.

The effect of high P loading (2.0 wt.% of $P_2O_5$) on the surface of HMS-based catalysts was different for the HDS of DBT [15] and the HDS of 4,6-DMDBT reactions [17]. Thus, contrary to HDS of DBT, the same high P loading (2.0 wt.% of $P_2O_5$) favored the catalytic behavior of CoMo/P/HMS sulfide catalysts in the HDS of 4,6-DMDBT reaction. The activity enhancement was associated with the larger sulfidation degree of cobalt species as confirmed by XPS analysis. However, both phosphorus promotion in the HDS of DBT [15] and inhibition in the HDS of 4,6-DMDBT [17] were observed for the CoMoS/P(x)/HMS catalysts prepared by simultaneous impregnation (**Figure 6**). Thus, it is obvious that the effect of modification of HMS substrate with P on the catalyst activity is contradictory. The drop in activity in the HDS of DBT reaction over CoMo/P-HMS sulfide catalyst (2.0 wt.% of P) was explained in terms of the much lower specific surface area and the presence of a large surface concentration of unsulfided $Co^{2+}$ species on the P-containing sample [16].
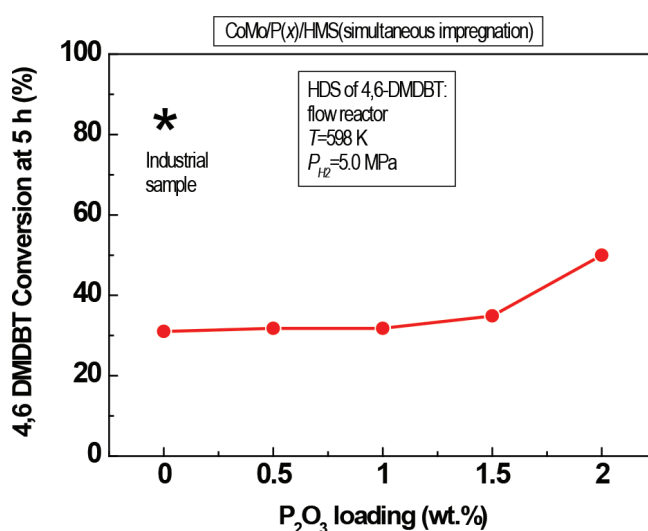


**Figure 6.** Influence of P loading on the activity of CoMo/HMS sulfide catalysts in the HDS of 4,6-DMDBT. The catalysts were prepared by simultaneous impregnation. As reference, the 4,6-DMDBT conversion data of an industrial sample is included (adapted from Nava et al. [17] with permission from Elsevier).

The promotional P effect was also observed for P/SBA-16-supported NiMoW catalysts when used in both HDS of DBT and 4,6-DMDBT reactions [25]. For both reactions, the catalyst activity plotted against P loading exhibited a volcano-type curve. The volcano-curve activity trend reported for NiMoW/P/SBA-16 sulfide catalysts was attributed to the promotional effect of P leading to an increase of the dispersion (from HRTEM). However, the catalyst loaded with the largest amount of phosphorus (1.6 wt.%) exhibited a drop of HDS activity with respect to its P-free counterpart. The low HDS activity of the P-free counterpart with respect to the P-containing NiMoW/SBA-16 sulfide catalysts was explained in terms of the formation of the "onion-type" Mo(W)$S_2$ phases (*vide supra* **Figure 3**), in good agreement with the study by Huang et al. [51]. This is because the "onion-type" phase exhibits the closed shell structure of $MoS_2$ which displays a low amount of HDS active edge sites. Regardless of the P content, DBT and 4,6-DMDBT transformation over NiMoW/P/SBA-16 catalysts occurred through two parallel routes of hydrogenation (HYD) and direct desulfurization (DDS) reaction routes [25].

**Figure 7** shows the influence of P loading on the HYD/DDS selectivity ratio in this reaction over NiMoW/P/SBA-16 sulfide catalysts. As seen in this figure, the catalysts modified with P exhibited the enhancement of HYD route of the DBT HDS reaction, in good agreement with those observed for CoMoW/SBA-16 by Huirache-Acuña et al. [24].
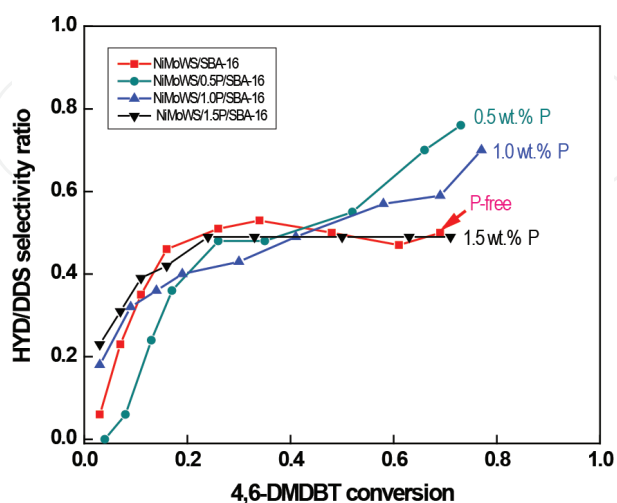


**Figure 7.** Influence of P loading on the HYD/DDS selectivity ratio in the HDS of 4,6-DMDBT over NiMoW/P/SBA-16 sulfide catalysts (adapted from Guzman et al. [25] with permission from Elsevier). Reaction conditions were: a batch reactor, $T = 320°C$, $P = 5.0$ MPa, and $t = 0.5$ h.

In order to promote the migration of the methyl groups in the aromatic ring of 4,6-DMDBT, attempts were made to enhance the acid properties of support by the substitution of $Si^{4+}$ atoms by $Al^{3+}$ or $Ti^{4+}$ ions in the pore walls of mesoporous silicas. The effect of support modification with both P and $Al^{3+}$ (or $Ti^{4+}$) on the activity of OMS-based catalysts has been studied by several authors [13, 14, 21, 22, 34]. In all these studies, P was incorporated by impregnation of the parent substrate with $H_3PO_4$. Zepeda et al. [21] investigated the catalytic response of CoMo/P/HMS-Ti sulfide catalysts in the HDS of DBT reaction carried out in a batch reactor at 320°C and total $H_2$ pressure of 5.5 MPa. It was found that HDS activity strongly increased upon P loading up to 0.64 wt.% of $P_2O_5$. The most active catalyst was 3.7 times more active than a commercial reference one and 2.4 times more active than its P-free counterpart. From the catalyst characterization, this was explained as due to specific electronic properties of the active phases and the largest Mo surface exposure on the support surface (from XPS).

The effect of phosphorus loading was also studied for sulfided NiMo/P/HMS-Al catalysts by Zepeda et al. [22]. For both thiophene and 4,6-DMDBT HDS reactions, the activity of P-loaded sulfide catalysts against $P_2O_5$ loading follow a volcano-shaped curve. The highest activity was exhibited by the catalyst doped with an optimized amount of P (1.0 wt.% of $P_2O_5$). This was explained in terms of the appropriate balance of active phase dispersion and largest hydrogenation ability of the catalysts. Indeed, a linear dependence was observed between catalyst activity and the active phase dispersion derived from $H_2$ chemisorption. The detrimental effect of a large P loading (1.5 and 2.0 wt.% of $P_2O_5$) on the HDS activity of NiMo/P/HMS-Al catalysts was attributed to a large decrease in their specific surface area with respect to P-free cata-

lysts [22]. Moreover, the decrease in the active phase dispersion of the catalysts was consistent with a more difficult sulfidation of the support-attached tetrahedral Mo species, as confirmed by combined DRS UV-vis and temperature-programmed sulfidation (TPS) experiments of the oxide precursors.

### 8.2. Effect of the catalyst preparation method

The most widely used preparation method of the Co(Ni)-promoted Mo(W) catalysts is the wetness impregnation of P/OMS supports with metal salt precursors. The direct preparation based on the dissolution of ammonium heptamolybdate in the presence of phosphoric acid has also been reported. In such cases, phosphorus acid is first added to an aqueous solution of ammonium heptamolybdate before adding nickel (cobalt) [50].

The Co(Ni)-promoted Mo-based catalysts are usually prepared by simultaneous or sequential impregnation of the P/OMS substrates with Co(Ni) and molybdenum salts solutions. The influence of both methods on the HDS activity of phosphate-containing CoMo/P/HMS sulfide was studied by Nava et al. [15]. The effect of the catalyst preparation method on the HDS activity of that catalysts is shown in **Figure 5** (*vide supra*).
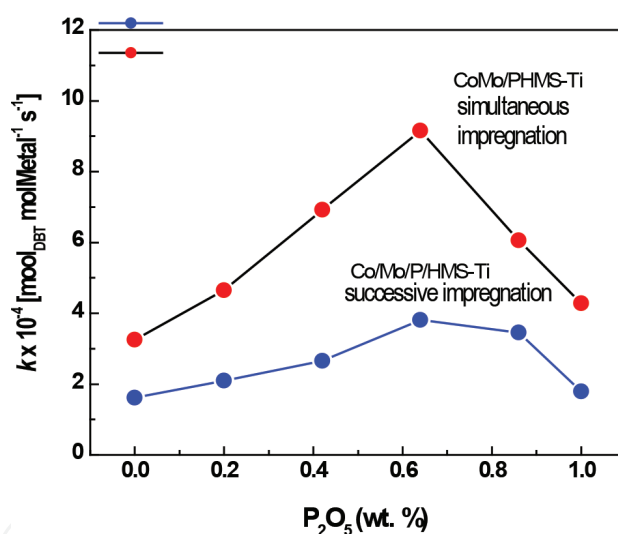


**Figure 8.** Influence of the catalyst preparation method and support modification with P on the pseudo-first reaction rate constants in the HDS of DBT over sulfided Co/Mo/P(*x*)/HMS-Ti and CoMo/P(*x*)/HMS-Ti catalysts (adapted from Pawelec et al. [13] with permission from Elsevier).

The influence of the catalyst preparation method (successive vs. simultaneous impregnation) on the HDS activity of P-containing CoMo/HMS-Ti sulfide catalysts in the HDS of DBT reaction was studied by Pawelec et al. [13]. **Figure 8** shows the reaction rate constants calculated from the DBT conversion at reaction time of 4 h. As seen in this figure, the simultaneous P/HMS-Ti support impregnation with Co and Mo precursors led to a larger enhancement of HDS activity than that prepared by successive impregnation. For both catalyst series, the promotion of P was not linear and the optimum P loading was found to be close to 0.64 wt.% ($P_2O_5$ content). Importantly, it was found that the catalyst supported on the P/HMS-Ti substrate having an

optimized P loading (0.64 wt.% of $P_2O_5$), which was prepared by simultaneous impregnation, exhibited a larger HDS activity than an industrial catalyst having the same formulation.

The effect of the catalyst preparation method and support modification with P on the reaction mechanism of the 4,6-DMDBT transformation over CoMo/P/HMS-Ti sulfide catalysts was studied by Pawelec et al. [14]. This is contrary to the NiMo/P/HMS-Ti sulfide catalysts which showed the 4,6-DMDBT transformation via HYD and DDS reaction routes [22]. The post-synthesis modification of HMS-Ti with phosphorus led to an enhancement of dealkylation and isomerization routes of 4,6-DMDBT transformation over the CoMo/P/HMS-Ti sulfide catalysts [14].

## 8.3. Effect of phosphorus addition on coke formation

By means of the TPO/TG analysis of the spent P-free and P-containing CoMo/HMS catalysts tested in HDS of DBT, Nava et al. [17] observed that P-containing catalysts were more susceptible to coking and produced more hydrogen-rich coke than the P-free counterpart. Besides the larger coke formation, the CoMo/HMS catalyst with the largest P loading (2.0 wt. % of $P_2O_3$) exhibited the best performance in the HDS reaction. From the catalyst characterization, this was ascribed to a proper balance between active phase dispersion and the lowest deactivation among the catalysts studied. This is because, besides the coke formation, other factors might contribute to catalyst deactivation. Thus, the opposite trend observed for the catalyst stability and the amount of coke formed strongly suggested that the presence of phosphate species on the support surface could avoid particles sintering during on-stream conditions. Moreover, the presence of phosphate species on the support surface helps maintain a large surface area of the supported catalysts, as observed for the alumina-supported ones [46, 47]. This means that an optimum loading of phosphorus may increase the longevity of the catalysts. However, the introduction of high amounts of phosphate led to an increase in the catalyst acidity, as confirmed for the NiMo/Al-HMS-P catalysts by Zepeda et al. [22], leading to promotion of coke formation. In this context, Stanislaus et al. [52] demonstrated that the strong acid sites of the alumina substrate, which are important in coking, are progressively poisoned by phosphate addition. However, the introduction of a high amount of phosphate created medium strength acid sites, and in turn, the total acidity of support increases. As a consequence, one might expect that the coking might also increase.

The influence of the support morphology (SBA-15 vs. SBA-16) and their modification with phosphate on the coking behavior of sulfided CoMoW catalysts was investigated by Huirache-Acuña et al. [24]. In general, it was reported that the spent SBA-16-based catalysts showed a lower coke formation in the hydrodesulfurization (HDS) of dibenzothiophene (DBT) than their SBA-15-based counterparts. This is because the phosphate incorporation to the SBA-16 support led to a decrease in coke formation in the final catalysts, as opposite to the behavior of the SBA-15-based counterparts. Interestingly, it was found that the phosphate addition to SBA-15 substrate led to an increase in coke formation, whereas for the SBA-16-based catalysts, the incorporation of a large amount of phosphate (1.5 and 2 wt.% of P) followed an opposite trend. Since a correlation was found between the amount of weak and medium strength acid sites and the amount of coke, this might indicate that coke formation on this sample occurs on the

acid sites that are located in the close vicinity of CUS sits. Multipoint centers for coke adsorption have been suggested as the sites that are first poisoned by coke [53].

Summarizing, regardless of the support morphology, the optimization of P loading seems to be an important parameter in the design of the active hydrotreating catalysts supported on the ordered mesoporous siliceous substrates. This is because phosphorus content usually affects the active phase dispersion, the catalyst acidity, the metal-support interaction, and the number of active sites. It was found that the support modification with P affected the following aspects of the final catalyst: (i) its structural and textural properties ($S_{BET}$); (ii) its acidity, and (iii) the formation of different phases in the oxide precursors. However, the addition of phosphorus to mesoporous siliceous materials has a nonlinear effect on the catalytic activity because the incorporation of a large amount of phosphorus (>0.1 wt.%) led to a decrease in the HDS activity of hydrotreating catalysts. This is probably due to a weakening of the metal-support interaction leading to a lower dispersion of the metal oxide phases, similar to that observed for alumina-supported hydrotreating catalysts [3].

# 9. Conclusions

On the basis of the present revision on the effect of modification of mesoporous silica materials by -$PO_3H_2$ groups for the activity of sulfides catalysts in different hydrotreating reactions, the following conclusions can be drawn:

i. The effect of the modification of the mesoporous silicas with phosphorus strongly depends on the P loading and method of its incorporation.

ii. The amount of phosphorus should be optimized and the best activity results are obtained for the catalysts modified with 1 wt.% of P.

iii. Support functionalization with -$PO_3H_2$ groups by post-synthesis method increases the substrate acidity without deterioration of its morphology.

iv. The catalytic behavior of sulfided catalysts depends strongly on the characteristics of their oxide precursors. Thus, a linear correlation was found between the presence of irregular (bankrupt) oxidized Mo particles in the oxide precursors and the catalytic response.

v. The deposition of oxide Co and Mo precursors by simultaneous impregnation led to more active HDS catalysts than their deposition on the support surface by successive impregnation method. This is because the former method led to a larger BET-specific surface area, a larger amount of $Co^{2+}$ ions having octahedral symmetry, and a larger amount of Mo species having Mo=$O_T$ bonds.

vi. Irrespective of the catalyst preparation method, the presence of phosphate species on the surface of HMS-Ti substrates has a beneficial effect on the HDS activity of the catalysts because of the enhanced formation of octahedral $Co^{2+}$ species and irregular $Mo^{6+}$ particles in the oxide precursors.

**vii.** Compared with classical $\gamma$-$Al_2O_3$, the HMS support modified with both Ti (Si/Ti molar ratio of 40) and phosphate shows appropriate textural characteristics to be used as support for HDS catalysts.

## Acknowledgements

## Author details

Rafael Huirache-Acuña[1*], Eric M. Rivera-Muñoz[2], Trino A. Zepeda[3], Rufino Nava[4] and Barbara Pawelec[5]

*Address all correspondence to: rafael_huirache@yahoo.it

1 Chemical Engineering Faculty, Michoacan University of Saint Nicholas of Hidalgo, Morelia, Michoacán, México

2 Center of Applied Physics and Advanced Technology, National Autonomous University of Mexico, Querétaro, Qro., México

3 Center of Nanoscience and Nanotechnology, National Autonomous University of Mexico, Ensenada, BC, México

4 Engineering Faculty, Autonomous University of Querétaro, Querétaro, Qro., México

5 Institute of Catalysis and Petroleochemistry of the Spanish National Research Council, Cantoblanco, Madrid, Spain

## References

[1] Vasudevan P.T., Fierro J.L.G. *Catalysis Review-Science Engineering*. 1996; 38: 161–188.

[2] Breysse M., Afanasiev P, Geantet C., Vrinat M. *Catalysis Today*. 2003; 86: 5–16. DOI: 10.1016/S0920-5861/(03)00400-0.

[3] Iwamoto R., Grimblot J. *Advances in Catalysis*. 2000; 44: 417–503. DOI: 10.1016/S0360-0564(08)60516-7.

[4] Lai, W.F., Hamilton M.A., McCarthy S.J. WO2013059176 A1. 2013.

[5] Fierro J.L.G, López Agudo A., Esquivel N., López Cordero R. *Applied Catalysis* 1989; 48:353–363.

[6] Robinson, W.R.A.M., van Gestel J.N.M., Korányi T.I., Eijsbouts, S., van der Kraan A.M., van Veen, J.A.R., de Beer V.H.J. *Journal of Catalysis*. 1996; 161:539–550. No. 0021-9517/96. No. 0166-9834.

[7] Topsøe H., Clausen B.S., Massoth F.E. in: J.R. Anderson, M. Boudart (Eds.) Hydrotreating Catalysts. Science and Technology, Springer-Verlang, Berlin, 1996. Vol. 11.

[8] Gishti K., Iannibello A., Marengo S., Morelli G., Tittarelli P. *Applied Catalysis*. 1984; 12: 381–393. 0166-9834/84.

[9] Van der Bij H.E., Weckhuysen B.M. *Chemical Society Reviews*. 2015; 44: 7406–7428. DOI: 10.1039/C5CS00109A.

[10] Korányi T.I. *Applied Catalysis A: General*. 2003; 239: 253–267.PII: S092-860X(02)00390-3.

[11] Herrera J.M., Reyes J., Roquero P., Klimova T. *Microporous and Mesoporous Materials*, 2005; 83: 283–291.DOI: 10.1016/j.micro.meso.2005.05.010.

[12] Zepeda T.A., Pawelec B., Obeso-Estrella R., Díaz de León J.N., Fuentes S., Alonso-Nuñez G., Fierro J.L.G. *Applied Catalysis B: Environmental* 2016; 180: 569–579. DOI: 10.1016/j.apcatb.2015.07.013.

[13] Pawelec B., Halachev T., Olivas A., Zepeda T.A. *Applied Catalysis A: General* 2008; 348: 30–41. DOI: 10.1016/j.acata.2008.06.014.

[14] Pawelec B., Fierro J.L.G., Montesinos A., Zepeda T.A. *Applied Catalysis B: Environmental* 2008; 80: 1–14. DOI: 10.1016/j.apcatb.2007.10.039.

[15] Nava R., Morales J., Alonso G., Ornelas C., Pawelec B., Fierro J.L.G. *Applied Catalysis A: General* 2007; 321: 58–70. DOI: 10.1016/j.acata.2007.01.038.

[16] Nava R., Pawelec B., Morales J., Ortega R.A., Fierro J.L.G. *Microporous and Mesoporous Materials*, 2009; 118: 189–201. DOI: 10.1016/j-micromeso.2008.08.045.

[17] Nava R., Infantes-Molina A., Castaño P., Guil-López R., Pawelec B. *Fuel*, 2011 90: 2726–2737. DOI: 10.1016/j.fuel.2011.03.049.

[18] Kresge J.S., Leonowicz M.E., Roth W.J., Vartuli J.C., Beck J.S. *Nature* 1992; 359: 710–712. DOI: 10.1038/359710a0.

[19] Tanev P.T., Chibwe M., Pinnavaia T.J. *Nature*, 1994; 368: 321–323. DOI: 10.1038/368321a0.

[20] Tanev P.T., Pinnavaia T.J. *Chemistry of Materials* 1996; 8: 2068–2079. DOI: 10.1021/cm950549a.

[21] Zepeda T.A., Pawelec B., Fierro J.L.G., Montesinos A., Olivas A., Fuentes S., Hala-chev T. *Microporous and Mesoporous Materials* 2008; 111: 493–506. DOI: 10.1016/j.micromeso.2007.08.027.

[22] Zepeda T.A., Infantes-Molina A., Díaz de León J.N., Fuentes S., Alonso-Núñez G., Torres-Otañez G., Pawelec B. *Applied Catalysis A: General* 2014; 484, 108–121. DOI: 10.1016/j.apcatb.2014.06.033.

[23] Zhao D., Feng J., Huo Q., Melosh N., Fredrickson G.H., Chmelka B.F., Stucky G.D. *Science* 1998; 279: 548–552.

[24] Huirache-Acuña R., Pawelec B., Rivera-Muñoz E., Nava R., Espino J., Fierro J.L.G. *Applied Catalysis B: Environmental*, 2009; 92: 168–184. DOI: 10.1016/j.apcatb.2009.07.012.

[25] Guzmán M.A., Huirache-Acuña R., Loricera C.V., Hernández J.R., Díaz de León J.N., de los Reyes J.A., Pawelec B. *Fuel* 2013; 103: 321–333. DOI: 10.1016/j.fuel.2012.07.005

[26] Loricera C.V., Pawelec B., Infantes-Molina A., Alvarez-Galván M.C., Huirache-Acuña R., Nava R., Fierro J.L.G. *Catalysis Today* 2011; 172: 103–110. DOI: 10.10916/j.cattod.2011.02.037.

[27] Sakamoto Y, Keneda M., Teresaki O., Zhao D.Y., Kim J.M., Stucky G., Shin H.J., Ryoo R. *Nature* 2000; 408: 449–453. DOI:10.1038/35044040.

[28] Pitchumani R., Li W., Coppens M.-O. *Catalysis Today* 2005; 105: 618–622. DOI: 10.1016/j.cattod.2005.06.002.

[29] Tagaya M., Kobayashi K., Nishikawa M. *Materials Letters* 2016; 164:651–654. DOI: 10.1016./j.matlet.2015.11.070.

[30] Vallet-Regí M., Izquierdo-Barba I., Rámila A., Pérez-Pariente J., Babonneau F., González-Calbet *Solid State Science*. 2005; 7: 233–237. DOI: 10.1016/j.solidstatesciences.2004.10.038.

[31] Kawi S., Shen S.C., Chew P.L. *Journal of Materials Chemistry*. 2002; 12, 1582–1586. DOI: 10.1039/b107795n.

[32] González M.D., Salagre P., Mokaya R., Cesteros Y. *Catalysis Today* 2014; 227: 171-178. DOI: 10.1016/j.cattod.2013.10.029.

[33] Gontier, S., Tuel A. *Zeolites* 1995; 15:601–610. DOI:10.1016/0144-2449(95)00028-5.

[34] Hernández A., Escobar J., Pacheco, J.G., de los Reyes J.A., Barrera, M.C. *Journal of the Mexican Chemical Society*, 2004; 48: 260–268.

[35] Van der Bij H.E., Cicmil D., Wang J., Meirer F., de Groot F.M.F., Weckhuysen B.M. *Journal of American Chemical Society* 2014; 136(51): 17774–17787. doi: 10.1021/ja508545m.

[36] Lezcano-Gonzalez I., Deka U., van der Bij H.E., Paalanen P., Arstad B., Weckhuysen B.M., Beale A.M. *Applied Catalysis B: Environmental* 2014; 154-155:339–349. DOI: 10.1016/j.apcatb.2014.02.037.

[37]   Van der Bij H.E., Weckhuysen B.M. *Physical Chemistry and Chemical Physics* 2014; 16: 9892–9903. DOI: 10.1039/c3cp54791d.

[38]   Van der Bij H.E., Aramburo L.R., Arstad B., Dynes J.J., Wang J., Weckhuysen B.M. *ChemPhysChem*. 2014; 15: 283–292. DOI: 10.1002/cphc.201300910.

[39]   Shon J.K., Yuan X., Ko C.H., Ik Lee H., Thakur S.S., Kang M., Kang M.S., Li D., Kim J.N., Kim J.M. *Journal of Industrial Engineering Chemistry*. 2007; 13(7): 1201–1207.

[40]   El Mourabit S., Guillot M., Toquer G., Cambedouzou J., Goettmann F., Grandjean A. *RSC Advances* 2012; 2: 10916–10924. DOI: 10.1039/c2ra21569a.

[41]   Xiong L., Yang Y., Shi J., Nogami M. *Microporous and Mesoporous Materials*. 2008; 111: 343–349. DOI: 10.1016/j.micromeso.2007.08.016.

[42]   Spanos N., Lycourghiotis A. *Journal of Colloid Interface Science*. 1995; 171: 306–318. DOI: 10.1006/jcis.1995.1185.

[43]   Oyama S.T. *Journal of Catalysis* 2003; 216: 343–352. DOI: 10.1016/S0021-9517(02)00069-6.

[44]   Huirache-Acuña R., Nava R., Peza-Ledesma C.L., Lara-Romero J., Alonso-Núñez G., Pawelec B., Rivera-Muñoz E.M. *Materials* 2013; 6:4139–4167.

[45]   Wang Y., Shen B., Hao K., Li J., Wang L.; Feng B., Guo Q. Catalysis Communications 2012; 25: 59–63. DOI: 10.1016/j.catcom.2012.04.004.

[46]   Lewis J.M., Kydd R.A. *Journal of Catalysis*, 1991; 132: 465–471. DOI: 10.1016/0021-9517(91)90163-X.

[47]   Lewis J.M., Kydd R.A., Boorman P.M., van Rhyn P.H. *Applied Catalysis A: General*, 1992; 84: 103–121. DOI: 10.1016/0926-860X(92)80110-X.

[48]   Lű, R., Cao, Z., Wang, S. *THEOCHEM*, 2008; 865:1–7. DOI: 10.1016/j.theochem. 2008.06.009.

[49]   Halachev T., Nava R., Dimitrov L. *Applied Catalysis A: General*, 1998; 169: 11–117. *PII* S0926-860X(97)00374-8.

[50]   Nava H, Espino, J., Berhault G., Alonso-Nuñez G. *Applied Catalysis A: General*, 2006; 302: 177–184. DOI: 10.1016/j.apcata.2005.12.025

[51]   Huang L., Li Q. *Chemistry Letters*, 1999; 28(8): 829–830. DOI: 10.1246/cl.1999.829

[52]   Stanislaus A., Absi-Halabi M., Al-Doloma K. *Applied Catalysis* 1988; 39: 239–253. DOI: 10.1016/S0166-9834(00)80952-5.

[53]   Ione K.G., Echeviskii G.V., Nosyreva G.N. *Journal of Catalysis*. 1984; 85: 287–294. No. 0021-951718.